Local Ferromagnetic Resonance Imaging with Magnetic Resonance Force Microscopy

Yu. Obukhov,[1] D. V. Pelekhov,[1] J. Kim,[1] P. Banerjee,[1] I. Martin,[2] E. Nazaretski,[2] R. Movshovich,[2] S. An,[1] T. J. Gramila,[1] S. Batra,[3] and P. C. Hammel[1,*]

[1]*Department of Physics, The Ohio State University, Columbus, Ohio, 43210, USA*
[2]*Los Alamos National Laboratory, Los Alamos, New Mexico, 87545, USA*
[3]*Seagate Research, 1251 Waterfront Place, Pittsburgh, Pennsylvania 15222, USA*

(Received 27 January 2008; published 14 May 2008)

We report nanoscale scanned probe ferromagnetic resonance force microscopy (FMRFM) imaging of individual ferromagnetic microstructures. This reveals the mechanism for high spatial resolution in FMRFM imaging: the strongly inhomogeneous local magnetic field of the cantilever mounted micromagnetic probe magnet used in FMRFM enables selective, local excitation of ferromagnetic resonance (FMR). This approach, demonstrated here in individual permalloy disks, is straightforwardly extended to excitation of localized FMR modes, and hence imaging in extended films.

DOI: 10.1103/PhysRevLett.100.197601 PACS numbers: 76.50.+g, 07.79.−v, 75.30.Ds, 75.75.+a

The demands of high density information storage and magnetoelectronics have fueled interest in understanding the properties of nanoscale magnets and have highlighted the need for tools capable of subsurface, high spatial resolution study and imaging of ferromagnets. Ferromagnetic resonance (FMR) [1] is a powerful technique for obtaining detailed information regarding the magnetic properties of microscale ferromagnetic systems. However, limited by its sensitivity, FMR can only be applied to large collections of nanoferromagnets. Magnetic resonance force microscopy (MRFM) detection of FMR (FMRFM) has been demonstrated in micron-scale magnets [2–5], and with single electron spin sensitivity [6], MRFM can detect signals from the smallest magnets.

In addition to high sensitivity, microscopic study requires a *mechanism for controllably defining the volume to be studied,* but so far, no mechanism for so confining the FMR excitation is known. Magnetic resonance imaging (MRI), very powerful for paramagnetic systems, defines the resonant volume by means of an applied magnetic field gradient. This paradigm assumes weakly interacting spins for which the resonance frequency is a local function of applied field, independent of the state of neighboring spins—a condition not met in a ferromagnet.

Here we demonstrate that the localized magnetic field of the micromagnetic scanned probe tip employed for FMRFM can define the detected volume in a microscopic FMRFM experiment. We present images of individual micron-scale dots that reveal the mechanism by which an intense, localized magnetic field locally alters the FMR mode frequency. This provides a mechanism for spatially defining the volume in which an FMR mode is excited, and thus for high resolution imaging. This further means that the spatial variation of the FMR mode is encoded into a position-dependent spectral response, much as in MRI. This allows mode imaging with a spatial resolution set by the ratio of the spectral linewidth to the (potentially quite large) magnetic field gradient.

FMRFM was performed at $T = 4.2$ K on a square array of 50 nm thick, 2 μm diameter permalloy disks with 2.2 μm center to center spacing in a magnetic field H_{ext} adequate to saturate the magnetization (excitation frequency $\sim$8 GHz) applied perpendicular to the plane of the disks. The FMR signal is detected by a compliant cantilever with a high coercivity ($\gtrsim$1.5 T) SmCo micromagnetic probe tip fabricated by focused ion beam micromachining (moment 1.4×10^{-11} J/T). The FMR force signal is generated by amplitude modulation of the microwave field at the cantilever resonance frequency ($\approx$13 kHz); see Refs. [3,7,8] for details. FMR spectra are recorded by sweeping the external magnetic field H_{ext} at constant tip height and lateral position; position-dependent spectra are recorded as the tip position is scanned in either one [Fig. 2(a)] or two lateral dimensions [Fig. 2(b)], again at constant height.

As a consequence of the strong interactions between spins in a ferromagnet, resonant absorption of energy from the microwave magnetic field excites collective modes. In confined samples the allowed wave vectors of these magnetostatic modes are set by the sample dimensions (the mode amplitude is typically assumed to vanish at the boundary of the ferromagnet); these have been well studied in patterned magnetic films [9–11]. The spatial profile of m_{tr} in a thin ferromagnetic disk perpendicularly magnetized by a *uniform* external magnetic field $\mathbf{H}_{\text{ext}}$ is well described by the zeroth order Bessel function [12]: ${}^{n}m_{\text{tr}} = \mu_0 J_0(k_n \rho)$, where ρ is the distance from the center of the dot, a is the dot radius, α_n is the nth zero of J_0: $J_0(\alpha_n) = 0$ and $k_n = \alpha_n / a$ is the effective wave vector of the nth mode and μ_0 is the amplitude of the FMR mode.

A typical FMRFM spectrum recorded over the center of the disk is shown in Fig. 1. As the probe magnet is highly coercive, we record FMR spectra for both relative orientations of the probe magnetic moment $\mathbf{m}$ relative to $\mathbf{H}_{\text{ext}}$: parallel [Fig. 1(a)] and antiparallel [Fig. 1(b)].

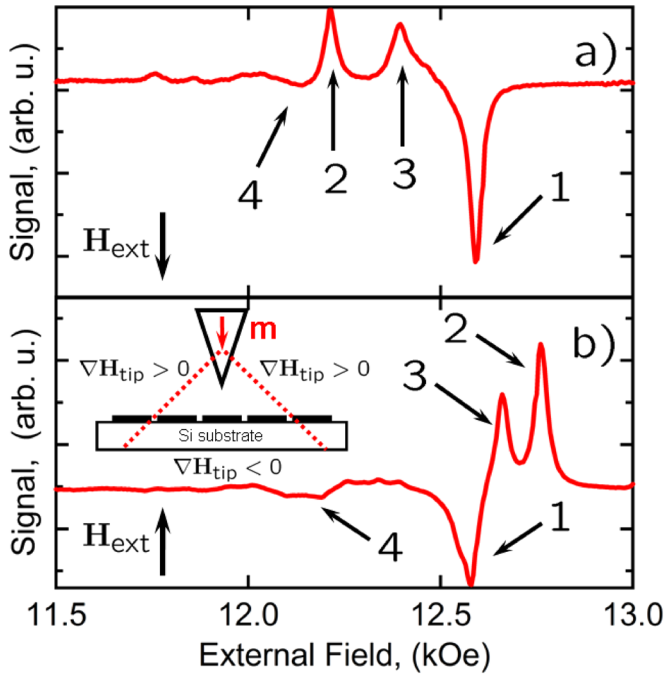

FIG. 1 (color online). FMRFM spectra of an array of 2 μm diameter permalloy dots acquired for two relative orientations of the probe magnet magnetic moment $\mathbf{m}$ relative to the external magnetic field $\mathbf{H}_{ext}$: parallel (a) and antiparallel (b). The first order TFR modes of the dots close to the micromagnetic probe are indicated as peaks 2 and 3, and the first and the second order ZFR magnetostatic modes are indicated (peak 1 and 4, respectively); these arise from dots far from the probe tip (tip-sample separation 200 nm). The spectra were acquired with the probe magnet located directly over the center of one of the dots as shown in the inset which also schematically indicates the dipolar gradient pattern of the probe magnet.

The spectra exhibit both positive and negative peaks. While the resonance fields of the negative-going peaks (labeled 1 and 4) are independent of the orientation of $\mathbf{H}_{ext}$ relative to $\mathbf{m}$, the resonance fields of the positive going peaks (2 and 3) are not. The negative peaks originate from dots far to the side of the tip where its localized magnetic field $\mathbf{H}_{tip}$ is so small it does not affect the mode; peak 1 is the first ($n = 1$) magnetostatic mode and 4 is the $n = 2$ mode. Here and below we will refer to a signal of this kind as a zero tip field resonance (ZFR). The ≈ 400 G spacing between the first and the second ZFR modes agrees well with theoretical predictions [12].

The positive peaks 2 and 3 originate from the disks in the immediate vicinity of the tip and their shifts are sensitive to the orientation of $\mathbf{H}_{tip}$ relative to $\mathbf{H}_{ext}$. If parallel, $\mathbf{H}_{tip}$ and $\mathbf{H}_{ext}$ will complement each other creating a region of the stronger field beneath the probe magnet so these disks will resonate at *lower* values of H_{ext} than for the ZFR as shown in Fig. 1(a). If $\mathbf{H}_{tip}$ and $\mathbf{H}_{ext}$ are antiparallel the magnetic field directly under the probe is weaker so *higher* values of H_{ext} will be required as seen in Fig. 1(b). Henceforth we will refer to a signal strongly affected by the probe field as a tip field resonance (TFR).

The relative signs of the ZFR and TFR signals reflect the dependence of the MRFM force signal $F(t)$ on the gradient of the probe magnetic field $\nabla\mathbf{H}_{tip}$: $\mathbf{F}(t) = \int_V [\delta\mathbf{M}(\mathbf{r}, t) \cdot \nabla]\mathbf{H}_{tip}(\mathbf{r})d\mathbf{r}$, where $\delta\mathbf{M}(\mathbf{r})$ is that component of the static sample magnetization varying at the cantilever frequency in response to the amplitude modulated microwave excitation; the integration is over the entire sample. The dipolar nature of the probe magnetic field means the sign of the gradient $\nabla\mathbf{H}_{tip}$ and hence the force due to magnetization directly below the tip will be opposite to that arising from magnetization off to the side (Fig. 1, inset).

The influence of the localized tip field on the FMRFM is evident in images of the spatial variation of these resonance fields with the position of the tip as it is scanned over the disks. Figure 2(a) shows an example of such an image acquired by scanning the probe as indicated in Fig. 2(b) with the probe moment $\mathbf{m}$ parallel to $\mathbf{H}_{ext}$. The plot shows the behaviors mentioned earlier: the broad black line is the first order ZFR; it is independent of the probe position as expected.

The series of light colored arcs in Fig. 2(a) show the tip-position-dependent FMR modes, i.e., the TFR modes. The most strongly shifted arcs correspond to the TFR signals from the disk directly beneath the probe magnet [as shown

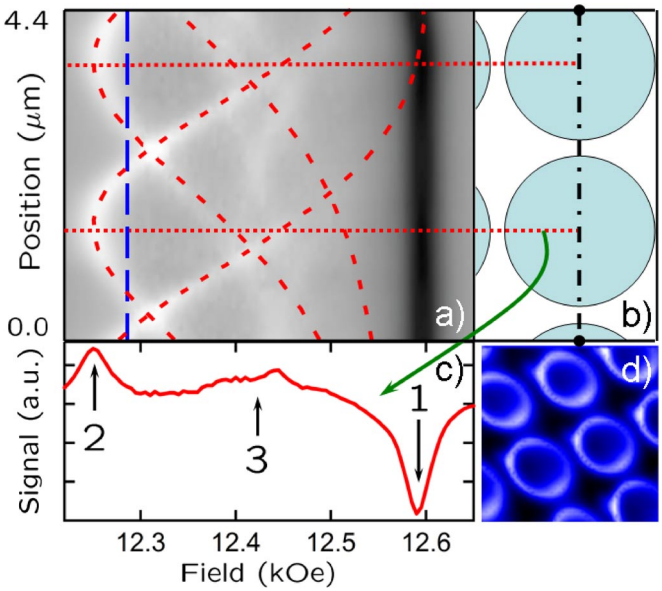

FIG. 2 (color online). (a) Field-position scan: FMR spectra recorded by sweeping the external magnetic field H_{ext} and spatially scanning the probe along the one-dimensional trajectory indicated by the dash-dotted line across the diagram of the dots in panel (tip-sample separation is 200 nm). (b) The red dashed curves in (a) show the analytically calculated dependence of the TFR resonance field on probe position; these agree excellently with the experimental data. (c) Spectrum extracted from image (a) with the tip located over the center of the upper dot [see panel (b)]. Numerical labels are as in Fig. 1. (d) Experimental fixed-field ($H_{ext} = 12.28$ kG) 2D image (4.8 μm $\times$ 4.8 μm) of the spatial variation of the FMRFM signal.

in Fig. 2(b)]. The maximum shift of the TFR signal occurs when the probe magnet is positioned directly over the center of a disk. The shift decreases as the probe moves away from the center of the disk, and the TFR mode eventually merges with the ZFR signal. The less-shifted TFR signals arise from the rows of disks adjacent to that immediately under the tip where probe magnetic field is weaker. The 2D image shown in Fig. 2(d) shows the variation of the FMR signal intensity as the tip is scanned at constant applied field $\mathbf{H}_{\text{ext}}$. The small deviation from the circular symmetry of the signal is due to a lateral component of tip magnetization.

The theory of FMR must be augmented to describe the scanned probe FMR experiments presented here in which the field of micromagnetic tip is strongly position dependent. Since analytical solution of the equations of motion for arbitrary sample geometry in the presence of a *nonuniform* magnetic field $H_{\text{eff}}(\mathbf{r})$ is not generally possible, we have solved them numerically to gain insight into this important problem [13]. Using the approach outlined in Ref. [14], we proceed by linearizing the Landau-Lifshitz equation and finding the eigenvalues and the eigenstates of the resulting matrix equation. Further detail is available in Ref. [13]. When applied to the case of uniform magnetic field [see Figs. 3(a) and 3(c)], this approach agrees accurately with analytical calculations [12].

Panel (b) in Fig. 3 shows the local mode defined by the intense localized field of the tip. This local mode provides the basis for high resolution FMR imaging. To obtain local magnetic information with high spatial resolution, the resonant volume must be confined since the FMR response is determined collectively by all of the resonant magnetization. The key to generating a local FMR mode confined to the region beneath the micromagnetic tip is a sufficiently strong tip field. This enables FMRFM to provide local, high resolution magnetic characterization of an extended film, a unique capability for studies in nanomagnetics and magnetoelectronics.

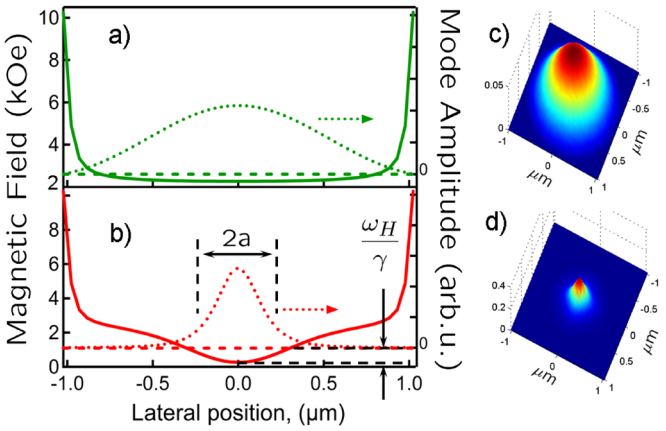

FIG. 3 (color online). Numerically calculated spatial profile of m_{tr} for the first order FMR mode excited in a 2 μm diameter, 50 nm thick Py disk ($4\pi M_s = 11$ kG, $H_{\text{ext}} = 13$ kG) in (a) a uniform external field and (b) in the presence of the field from a 1 μm diameter spherical magnet ($4\pi M_s = 11.3$ kG) located 250 nm above the center of the disk. The magnetic moment of the probe magnet $\mathbf{m}$ is *antiparallel* to $\mathbf{H}_{\text{ext}}$. The mode is confined to the region of reduced field beneath the probe. The dotted line shows the mode amplitude along a line through the center of the dot; the corresponding magnitude of the total magnetic field H_{tot} is shown with solid line; the dashed line indicates the resonance field H_{res} of the mode. (c) and (d) are the corresponding 2D maps of m_{tr}.

The numerical results, while precise, call for an intuitive insight into the mechanism by which the tip field localizes magnetization dynamics. Consider the Landau-Lifshitz equation applied to a uniform, perpendicularly magnetized dot. We focus on the behavior of the small transverse precessing magnetization and the resulting transverse magnetic field: $\mathbf{m}_{\text{tr}}$ and $\mathbf{h}_{\text{tr}}$, respectively, and, for clarity, we ignore damping and omit second order terms (e.g., components of $\mathbf{h}_{\text{tr}}$ and $\mathbf{m}_{\text{tr}}$ perpendicular to the plane):

$$\frac{1}{\gamma}\frac{d\mathbf{M}}{dt} = [\mathbf{m}_{\text{tr}}(t) \times \mathbf{H}_{\text{eff}}] + [\mathbf{M}_s \times \mathbf{h}_{\text{tr}}(\mathbf{t})].$$

Here γ is the gyromagnetic ratio of the electron ($\gamma < 0$), $\mathbf{H}_{\text{eff}}$ is the effective magnetic field incorporating static external, demagnetizing, anisotropy, exchange and MRFM probe fields, M_s is the saturation magnetization and ω is the microwave excitation frequency.

A monochromatic microwave magnetic field is applied to excite a resonant mode. In order to be driven by this field the mode shape must be such that the precession frequency is *constant* throughout the sample, everywhere matching the microwave excitation frequency. We seek oscillatory solutions for $m_{\text{tr}}(t)$ noting that h_{tr} is a function of m_{tr}. For clarity we focus on the case where $\mathbf{m}_{\text{tr}} = (m_{\text{tr}}, im_{\text{tr}})$ and $\mathbf{h}_{\text{tr}} = -(h_{\text{tr}}, ih_{\text{tr}})$, but recognize that $H_{\text{eff}}(\mathbf{r})$ can be spatially nonuniform. In this case the FMR resonance frequency in the Herring-Kittel form [15] is

$$-\frac{1}{\gamma}\omega(\mathbf{r}) = H_{\text{eff}}(\mathbf{r}) + \frac{M_s h_{\text{tr}}(\mathbf{r})}{m_{\text{tr}}(\mathbf{r})} = H_{\text{res}}(\mathbf{r}). \qquad (1)$$

Conventional FMR theory assumes a uniform magnetic field (H_{eff} independent of $\mathbf{r}$). In this case the second term on the right-hand side (rhs) of Eq. (1) must be constant throughout the sample—this requirement determines the spatial variation of $m_{\text{tr}}(\mathbf{r})$ and hence $h_{\text{tr}}(\mathbf{r})$.

For a sufficiently weak magnetic field inhomogeneity ΔH (due, e.g., to the micromagnetic tip), the precessing magnetization $m_{\text{tr}}(\mathbf{r})$ in the second term on the rhs of Eq. (1) will adjust to keep the resonant frequency constant throughout the sample. However, this is only possible for ΔH sufficiently weak and delocalized that it can be accommodated by variation of the transverse demagnetizing field $h_{\text{tr}}(\mathbf{r})$. This field is limited by the finite magnetization of a particular region of the film (of thickness L and radius a), so it cannot exceed $\Delta H_{\text{max}} \simeq 2\pi M_s(L/a)$. In the case where ΔH, for instance due to our tip field, exceeds ΔH_{max} within this confined region, an FMR eigenmode localized

to this region by the tip field will result. Numerical simulations shown in Fig. 3(b) reveal such modes resulting when a 1 μm diameter probe magnet magnetized antiparallel to the applied field is located 250 nm above the center of a circular dot producing a region of weaker total magnetic field H_{eff} at the center of the dot [13].

Since the diameter of the tip is comparable to the 2 μm disks whose images are shown in Fig. 2, it does not strongly perturb the mode shape. Even so, exact analytical determination of $m_{\text{tr}}(\mathbf{r})$ is not generally possible. However, the resulting shift in the resonance frequency can be accurately estimated without knowing the altered mode shape using a perturbation approach. To first order, the shift in the resonant frequency due to a spatially varying tip field $H_{\text{tip}}(\mathbf{r})$ is the average of H_{tip} over the dot weighted by the spatial profile of the squared, normalized, oscillating transverse magnetization ${}^n m_{\text{tr}}$ of the unperturbed nth magnetostatic mode:

$$\frac{\Delta\omega_n(\mathbf{r}')}{\gamma} = -\frac{\int H_{\text{tip}}(\mathbf{r}'-\mathbf{r})[{}^n m_{\text{tr}}(\mathbf{r})]^2 d\mathbf{r}}{\int [{}^n m_{\text{tr}}(\mathbf{r})]^2 d\mathbf{r}}. \quad (2)$$

Equation (2) is valid for arbitrarily shaped structures having unperturbed eigenmodes ${}^n m_{\text{tr}}(\mathbf{r})$. This approach to estimating $\Delta\omega(\mathbf{r}')$, where $\mathbf{r}'$ is the position of the probe over the dot, is similar to that introduced [12,16] to improve estimates of the magnetostatic mode frequencies for cases where the spatial variation of the demagnetizing field cannot be neglected. Our calculation of $\Delta\omega(\mathbf{r}')$ agrees excellently with the our measured shift, as shown in Fig. 2(a).

According to Eq. (2) the distribution of the square of the transverse precessing magnetization $[{}^n m_{\text{tr}}(\mathbf{r}')]^2$ can be deconvolved if we know the tip field distribution $H_{\text{tip}}(\mathbf{r})$, hence the spatial variation of the FMR *frequency* enables direct imaging of FMR modes with resolution defined by spectral linewidth. For example, the spatial variation of the mode frequencies arising from two adjacent nanomagnets will be spatially resolved if they are separated by a distance greater than the ratio of the spectral linewidth to the lateral field gradient of the probe tip field. This resembles the frequency encoding approach used in conventional MRI. This is in contrast to an earlier method where resolution was set by tip dimensions because it relied on the spatial variation of the *force* acting on cantilever [17].

FMR provides detailed information about the magnetic properties of a sample; typically the magnetization throughout the entire sample participates in the resonant dynamics, and the resulting information reflects the global average of magnetic properties of the entire sample. To gain local information, the resonant magnetization must be confined. We have shown the mechanism by which a *local* FMR mode is stabilized by the intense, localized field of a micromagnetic tip. We have experimentally demonstrated this theory of the influence of the localized tip field with imaging experiments performed on 2 μm permalloy dots where the mode is localized by the dot boundary. In this case the dependence of the resonance field shift on the location of the micromagnetic tip is the spatial convolution of the field of the tip with the mode of the dot. This suggests an approach to imaging localized FMR modes based on Fourier deconvolution of the spatial variation of the mode frequency shift. Importantly, spatial resolution is not limited by the tip size but by the FMR linewidth and the field gradient of the tip. Line cuts through features shown in Fig. 2(d) exhibit edges whose 10%–90% widths are $\sim$250 nm wide, consistent with $\sim$70 G FMR linewidths and lateral gradients of 0.3 G/nm.

The ability to generate a local FMR mode points to a powerful means of imaging extended, buried ferromagnets. Based on scanned probe ferromagnetic resonance (FMRFM), the mode volume is defined by the localized field of the micromagnetic probe tip. This will enable the detailed information accessible through FMR measurements to be obtained with high spatial resolution determined by spectral linewidth and tip field gradient strength.

This work was supported by the U.S. Department of Energy through Grant No. DE-FG02-03ER46054.

*hammel@mps.ohio-state.edu

[1] S. V. Vonsovskii, *Ferromagnetic Resonance* (Pergamon, Oxford, New York, 1966).
[2] Z. Zhang, P. C. Hammel, and P. E. Wigen, Appl. Phys. Lett. **68**, 2005 (1996).
[3] T. Mewes *et al.*, Phys. Rev. B**74**, 144424 (2006).
[4] G. de Loubens *et al.*, Phys. Rev. Lett. **98**, 127601 (2007).
[5] K. Wago, D. Botkin, C. S. Yannoni, and D. Rugar, Appl. Phys. Lett. **72**, 2757 (1998).
[6] D. Rugar, R. Budakian, H. J. Mamin, and B. W. Chui, Nature (London) **430**, 329 (2004).
[7] P. C. Hammel and D. V. Pelekhov, in *Handbook of Magnetism and Advanced Magnetic Materials*, edited by H. Kronmüller and S. Parkin (John Wiley & Sons, Ltd., New York, NY, 2007), Vol. 5.
[8] Y. Obukhov, K. C. Fong, D. Daughton, and P. C. Hammel, J. Appl. Phys. **101**, 034315 (2007).
[9] R. W. Damon and H. van de Vaart, J. Appl. Phys. **36**, 3453 (1965).
[10] T. Yukawa and K. Abe, J. Appl. Phys. **45**, 3146 (1974).
[11] B. A. Kalinikos and A. N. Slavin, J. Phys. C **19**, 7013 (1986).
[12] G. N. Kakazei *et al.*, Appl. Phys. Lett. **85**, 443 (2004).
[13] D. V. Pelekhov, I. Martin, and P. C. Hammel, report, 2007 (to be published).
[14] A. E. LaBonte, J. Appl. Phys. **40**, 2450 (1969).
[15] C. Herring and C. Kittel, Phys. Rev. **81**, 869 (1951).
[16] K. Y. Guslienko, R. W. Chantrell, and A. N. Slavin, Phys. Rev. B **68**, 024422 (2003).
[17] M. M. Midzor *et al.*, J. Appl. Phys. **87**, 6493 (2000).